First author is Asst. Professor at the Department of Ceramic Engineering, NIT Rourkela, India and recently working as visiting scientist at Korea Research Institute of Standards and Science, Korea. Please cite this article as: D. Sarkar, M. C. Chu, and S. J Cho, "Ceramic - Polymer Nanocomposite: Alternate Choice of Bone", Journal of the Korean Ceramic Society, Vol. 45, No. 6, pp. 309-319, 2008.

Ceramic – Polymer Nanocomposite: Alternate Choice of Bone (Review)

Debasish Sarkar*, Min Cheol Chu and Seong Jai Cho

Nanometrology Center, Korea Research Institute of Standards and Science,
Yuseong-Gu, Daejon 305-340, SOUTH KOREA

Abstract

This study evaluates a range of materials that may be used to design prostheses for bone. It is found that nanocrystalline ceramic-polymer composite could be the best material for prosthetic bone with respect to biocompatibility, morphology, chemistry, and compatibility with the piezoelectric and mechanical behavior of long human bones, such as the femur.

Keyword: Bone, Prosthesis, Nanocomposite, Ceramic, Polymer

1. Introduction

In the past decade, three dimensional images of long bones such as the human femur have been commonly produced through computerized axial tomography (CT) scan and/or magnetic resonance imaging (MRI) data[1,2]. Direct conversion of these data into tailor-made bioimplants is a complex phenomenon, since it is not only dependent on the structure of the bone to be repaired or replaced, but is also closely associated with the composition, physical properties and anatomy of bone itself. In terms of structure, the typical human femur (Fig. 1) is primarily composed of two separate types of bone; compact or cortical and trabecular or cancellous or spongy bone, and is capable of accommodating several modes of stress, from a stationary condition to brisk walking[3]. Trabecular bone generally resides at the ends of bones and is porous (50-90%), lighter, and more energy absorbent than compact bone, providing effective cushioning for bone impact[4,5]. The longevity of bone is directly and/or indirectly related to bone composition and morphology; a typical bone matrix is bundles of collagen fibers infiltrated by a crystalline bioapatite mineral (45% by volume, 65% by weight), which resembles with synthetic hydroxyapatite (Hap), $Ca_{10}(PO_4)_6(OH)_2$[6-8]. The strength of

* Corresponding Author: sarkar@kriss.re.kr Tel: 82-42-8685858, Fax: 82-42-8685032

bone is also dependent on bone porosity and elasticity. The modulus of elasticity has considerable impact on the tensile and compressive strength of bone[9]. Currey observed that variations in the mineral content of bone have significant effects on its mechanical properties[10]. The elastic modulus, for instance, exhibits a monotonic increase with an increasing amount of mineralization (in this case, the weight of Ca^{++}/dry weight of bone); whereas, the strain at failure shows a monotonic decrease within the same range, while the bending strength and the area under the load-deformation curve reach a peak and then decline[11]. In-vivo, ligaments and tendons experience a combined loading of tensile stress and rubbing against bones or cartilage in a biological environment, which damage their surfaces and reduce their tensile strength. Hence, the major cause of failure of applied prostheses is due to the cellular events induced by the wear debris coming from the bearing surfaces[12,13]. Another factor to be considered the search for a material appropriate for use in bone prostheses is that the piezoelectricity of bone is an indistinct feature, i.e., mechanical stress results in electric polarization, the indirect effect, and an applied electric field causes strain, the converse effect[14,15]. A recent thorough mechano-transduction study suggests two different mechanisms are responsible for these effects: classical piezoelectricity due to the molecular asymmetry of collagen in dry bone, and fluid flow effects due to streaming potentials in wet bone[16]. Furthermore, the overall performance of bone also depends on sex[17]. For example, women have a wider pelvis than men; therefore, the quadriceps angle is greater in women (16^o) than in men (12^o), and the probability of rupture of women's knee anterior cruiciate ligament (ACL) is greater than for men[18]. Hence, a brief assessment of anatomy, chemistry and mechanical properties can inform the choice of alternative materials for the development of bioimplants.

2. Anatomy of the Femur bone

The histology of bone tissue offers a wealth of information to describe the anatomy of the femur bone. The complicated structure of bone exhibits anisotropic mechanical stress with respect to direction; hence, an introductory anatomical description on bone morphology is essential for material scientists.

Bone is a natural nanocomposite biomaterial with a complex hierarchical structure. Several organic – inorganic parts are encased in a strong collagen matrix with a blood circulation system. Fig 1a and Fig 1b display the structure of a typical hip bone, where the femur is attached as a ball-and-socket arrangement through a ligament. Fig 1c reveals the basic shape of the adult femur, which is strongly influenced by cortical and trabecular bone. It has been noted that prior to puberty the

epiphyseal disk itself converts into bone [19]. In this way, growth in bone girth happens prior to lengthwise development, stimulated by growth hormone and inhibited by estrogens and progesterone. The upper extremity of the femur presents a head, a neck, and a greater and a lesser trochanter. The femur is the longest and the strongest bone in the skeleton and is almost perfectly cylindrical for the greater part of its extent. In the erect posture it is not vertical, but inclines gradually downward and medialward, which facilitate the knee-joints being near the line of gravity of the body. A tissue called the periosteum covers the bone and brings in blood, lymph vessels and nerves. The central cavity of the femur is filled with bone marrow, where stem cells gives rise to all the types of blood cells.

As with all biological tissues, cortical bone contains many different structures that exist at many levels of scale. It is much denser than other types of bone and is found primarily in the shaft of long bones, forming the outer shell around cancellous bone at the ends of joints and around vertebrae. The cylindrical Haversian canal (~10μm to ~30μm in diameter) controls the transportation of blood, lymph vessels and nerves within cortical bone (Fig. 2a). Around the Haversian canal a group of concentric circular lamellae present, these lamellae are roughly 3μm to 7μm thick. Moreover, within and between lamellae are found small hollow gaps (~10μm in diameter) that are interconnected by small canaliculi (~1μm in diameter), usually running perpendicular to the circumference of the Haversian systems[19]. These gaps are called lacunae. The cortical bone is mainly composed of a three-layered structure packed with mineral and collagen fibrils. The first-level structure including the central blood vessel and surrounding concentric bone tissue is called an osteon. This first level is organized into woven bone, primary bone, plexiform bone, and secondary bone. One of the most intriguing second-level structural entities, from a mechanical point of view, is the cement line. Recent research suggests the cement lines are compliant, allowing them to absorb more energy and to arrest crack growth in bone[20]. Below this level, there is little quantitative information on the structure of cortical bone due to the difficulty of measuring both bone structure and mechanics at increasingly small levels. The third-level cortical bone structure may be separated into two basic types, lamellar and woven. Each type contains the type I collagen fiber/mineral composite. The lamellar and woven bones can be distinguished by the interior packing of their collagen fibers and minerals. In woven bone, the collagen fibers are randomly organized and very loosely packed. A thorough analysis of bone structure by Wiener and Traub illustrates the orientation of mineral collagen composite into lamellae[21]. A distinct gap or hole-zone can be seen within the packing of the collagen fibers, which are filled with crystal and developed with a hexagonal carbonate hydroxylapatite mineral called dahllite [22](Fig 2b). As shown in Fig 2c, the apatite crystals fit snugly within the ‘hole-zone’ of collagen fibers along the

side-to-side lattice. However, the packing of molecules in three dimensions is still a mystery. Fig. 3a illustrates that cancellous bone has an interconnecting porous architecture made up of curvilinear struts called trabeculae. The trabecular bone appears at the ends of long bones and the vertebral body. Its basic first-level structure is the trabeculae[23]. Trabecular bone contributes about 20% of the total skeletal mass within the body, while the remaining 80% is contributed by cortical bone. However, trabecular bone has a much greater surface area than cortical bone. Table 1 demonstrates the general features of cortical bone and trabecular bone, including volume fraction and surface area[24]. Except for the third level of the structure, there is no significant difference within cortical and trabecular bone. Trabecular bone is more compliant than cortical bone and is believed to distribute and dissipate the energy from articular contact loads.

Osteonal bone is the combination of concentric rings of bone tissue and blood vessels, as described in Fig 3b. The size and shape of bones not only changes during growth, but bones are continuously being remodeled in response to the stresses put on them throughout life. Approximately 10% of bone mass is removed and replaced each year. The remodeling of bone requires the simultaneous coordinated activities of osteoclasts and osteoblasts. Osteoclasts are multinucleated cells that are found on calcified bone surfaces. They degrade bone mineral and collagen by releasing mass and produce free calcium (Ca). The dissolved mineral is then released into the bloodstream in order to satisfy other bodily needs and to provide space for newer mineral deposits. In addition, osteoclasts release matrix-bound growth factors that attract osteoblasts. It is important to note that osteoclastic differentiation is usually balanced with bone formation to preserve bone architecture over many cycles of bone replacement. However, excess activity of osteoclasts (common after menopause in women) produces osteoporosis[19]. Bones become weaker as the cortical bone gets thinner and the spaces in spongy bone get larger, upsetting the normal remodelling balance and leading to a decrease in bone density and strength. Additionally, this destruction and formation of bone may produce wear particles and reduce the longevity of bone[12]. On the other end, osteoblasts are bone-forming cells that convert free calcium (Ca) to new bone. Osteoblasts contain an organic bone matrix that is heavily cross-linked with type-I collagen. The bone matrix is aligned along the lines of stress and osteoblasts deposit the hydroxyapatite mineral into the gaps of the matrix, resisting compression. According to Wolff's Law, osteocytes are responsible for growth and changes in the shape of bone, where they function as neurotransmitter cells and determine the response of bone to its mechanical environment[25]. Hence, the study of the hierarchical organization of bone has two purposes: first, it provides a consistent way to compare the properties of different tissues with respect to morphology and constituents; second, it provides a consistent scheme for defining levels for computational analysis of tissue micromechanics.

3. Femoral Minerals and Chemistry

The major constituents of bone tissue are minerals, organic material and water; the organic material is mainly collagen and the mineral is mainly HAp. Collagen makes bones flexible (elastic), mineral makes bones rigid, and water in the interstitial space stores nutrients. In an excellent ternary diagram, Rogers et. al demonstrate how the content of different constitutes are responsible for morphology and texture with respect to mammalian group and age[26]. As depicted in Fig 4, the content of the mineralogical phase (HAp) of human femur is well matched with earlier clinical data for human bone. In bone the nanocrystalline carbonated bioapatite mineral (dahllite) resembles synthetic hydroxyapatite [$Ca_{10}(PO_4)_6(OH)_2$], which is snugly arranged within collagen fibrils (Fig 2c). These collagen fibrils come together and form a collagen fiber, which is woven in a triple-helix to form a cylinder, 80-300nm x 1.5nm. Along with the content of these two inorganic and organic phases, water also contributes the durability of bone.

Research over the past two decades has focused on preparing synthetic HAp, since it closely resembles bone apatite and exhibits excellent osteoconductivity[27-29]. Usually, defective or poorly crystallized natural bioapatite exhibits broad diffraction lines, making it difficult to determine the exact phase through XRD technique. The remarkable property of synthetic hydroxyapatite is its bioactivity, particularly its ability, after implantation, to form chemical bonding with surrounding hard tissues. However, most synthetic apatites are formed via high temperature processes that result in a well-crystallized structure, which has low bioresorption in contrast to natural nanocrystalline bio-crystal apatite[30]. Recently, Dalconi et al compared the XRD patterns of foetal bone, adult bone and synthetic HAp, where the crystallographic analysis exhibits a relationship between the structures of bone bioapatite and synthetic hydroxyapatite[31]. Fig 5a illustrates that the diffraction lines of foetal bone samples are broader than those of adult bone, suggesting that the diffracting particles (crystallites) in the younger bone are smaller and/or have more defective crystal structure than adult bones. A typical crystal structure of synthetic HAp is represented in Fig 5b[32]. The unit cell parameters of foetal bioapatite are higher than those of synthetic HAp, whereas the reverse is true of adult bone apatite. Hence, the c/a ratio of HAp crystal could be seen as a function of age.

Synthetic HAp is an alternative choice as inorganic phase in bone, but requires a strong association with a mechanical load bearing and biocompatible fibril structure to produce a prosthesis. Presumably, the fibril array patterns are generally of four types, as indicated in Fig 6a – 6d: (a) parallel fibrils, (b) woven fiber structure, (c) plywood-like structure and (d) radial fibril arrays[33]. It has been observed that there are two possible collagen fibril arrangements in apatite crystal; parallel crystal

layers and non-parallel crystal layers. However, the fibrils are not distinct; they often merge with neighboring fibrils. In a similar manner, collagen, a common protein constituent of muscular arteries, provides great tensile strength in molecular and fiber form. Among the 20 types of collagen, the human body is mainly composed of collagens type I, II and III. Collagens type I and III are the major fibrillar collagens in blood vessels, where they represent 60% and 30% of vascular collagens, respectively[19]. The basic unit of fibrillar collagens is the triple helix formed by three intertwining amino-acid chains (Fig 6e) [34]. Each chain is roughly 330 amino acids long and the overall molecule, called tropocollagen, is 300nm long and has a diameter of roughly 1.5nm. The strength of collagen fibers is attributed to their stable intermolecular covalent bonds and cross linking between adjacent tropocollagen molecules. Cross-linking of collagen is a progressive and continuous process. However, the oxidative deamination, which decreases bone toughness with age, initiates the cross-linking through lysyl oxidase or due to a deficiency of copper ions[35]. The development and maintenance of bone mineral involves complex processes and a continuous turnover of mineral and organic parts deriving from metabolic activity, ageing and disease.

In short, human bone tissue is a composite comprised of a collagen matrix reinforced with 40–50vol% apatite crystals. The apatite crystals are elongated along the c-axis, with a preferred orientation in the directions of principal stress, such as the longitudinal anatomic axis of long bones. Several questions about the processes related to the evolution and growth of bone mineral still remain unanswered.

4. Piezoelectric Behavior of Bone

The less informative piezoelectric behavioral feature of bone is not clearly understood. In general, the deformation and subsequent separation of charge symmetry enhances the piezoelectric effect of the crystalline structure of bone[36]. The magnitude of the piezoelectric sensitivity coefficients of bone depends on frequency, direction of load, and relative humidity. The piezoelectric coefficient of bone is 0.7pC/N ($1N/m^2$ of stress produces $7x10^{-13}$ $Coulombs/m^2$ of charge on the surface), which is analogous to that of the asymmetric HAp crystal. Theoretical analyses of bone piezoelectricity are relevant to the topics of osteogenesis, bone remodeling, and bone metabolism. Osteogenesis is a formation process of bone initiated by connective tissue or cartilage. Osteogenesis promotion and bone metabolism regulation are mediated by electrical current generated by piezoelectric materials due to changing pressure. Electrical potential is generated between the compressive and tensile sides of bone when dry bone is subjected to a shearing force[37]. The developed negatively charged compression

side is associated with bone resorption and production. Hence, the magnitude of this charge is dependent upon the angle at which the load is applied and the charge symmetry of the crystals; thus, the lower the charge symmetry, the higher the piezoelectric effect upon deformation. However, this hypothesis is not supported in wet bone (in-vivo), as water molecules increase the symmetry of the charge[38]. Hence, to illustrate the mechanotransduction effect of wet bone, the entire mechanism has been categorized into four distinct steps: (1) mechanocoupling – the detection of environmental mechanical loads by sensory cells which, in turn, produce a local mechanical signal, (2) biochemical coupling – conversion of the local mechanical signal into a biochemical signal, (3) transmission of signal from the sensory cell to the effector (osteoblasts and osteoclasts) cell, and (4) effector cell response (i.e. bone production)[39]. Undoubtedly, the complete cycle is useful for understanding the piezoelectric mechanism of wet bone, where it can be stated that bone formation and resorption are linked to the magnitude, rate, and duration of the applied mechanical load.

5. Tribological Behavior of bone

A common problem with hip and knee arthroplasties frequently originates from the formation of wear debris through biological processes. Unbalanced osteoclast and osteoblast mechanisms provoke the loss of bone mineral and the subsequent formation of ultra fine debris particles that contribute to nano-scale tribological wear[13]. Recent studies confirm that wear particles profoundly alter the differentiation, maturation and function of osteoprogenitors, thereby contributing to the osteolytic process by decreasing bone formation. Modern progress in regenerative surgery raises the hope of repairing bone defects with a combination of biomaterials offering non-toxicity, growth factors contribute to the growth of bone growth factors, and tailor made properties. However, the surgical host bone grows in close contact to the implant and experiences some degree of micro-movement[40]. Under physiological loads, the biological thresholds for micro-movements at the bone implant interface are found to be in the range of 150 – 200μm. This displacement has deleterious effects on the function of prostheses. The resulting damages to bone or implant are related to low amplitude reciprocal oscillatory movement at the interface, and cause failures through an accumulation of micro cracks and other damages. This phenomena of wear induced by friction over small displacements is often referred to as fretting[41,42]. The mechanism of fretting damage to the living tissue of cortical bone is completely different from that occurring in metal, ceramic or polymer counterparts, and this wear mechanism at the bone interface can be considered, evaluated and compared using Hertz's method.

6. Choice of Material

Biocompatibility is a general term used to describe the adaptability of a material for exposure to the body or body-fluids. Biocompatible materials are generally non-inflammatory, non-toxic, non-carcinogenic and non-immunogenic, or have other suitable physical properties. The specific meaning of biocompatibility is dependent on a particular application or circumstance. In fact, there are no completely biocompatible materials. However, the continuous success of many medical devices and bone implants is contingent upon successful interaction of the biocompatible materials and various bodily tissues.

Traditionally, metallic materials, such as stainless steel, Ti alloys and cobalt–chromium alloys, have been widely used as bone implants in orthopedic applications[43-45]. The use of materials stiffer than bone tissue may lead to mechanical mismatch problems (e.g., stress shielding) between the implant and the adjacent bone tissue, where the integrity of the bone/implant interface may be compromised due to the resorption of bone tissue. On the other hand, most polymers, by themselves, do not posses sufficient mechanical properties to bear physiological loads. In order to minimize the stress-shielding effect while maximizing resistance to fractures, a polymer matrix based material is a possible alternative. Ceramic reinforced (e.g HAp) polymer composites for different load-bearing orthopedic applications have been significantly developed recently[46-49].

7. Prospects of Ceramic – Polymer Composite as bone

The human femur bone is a classical example of a nano-composite material, having strength that is higher than either of its components, apatite or collagen. The introductory part of the paper illustrated the anistopic mechanical response of bone Shortly, the failure mode of bone under circumstances of catastrophic overload is directly related to the loading mode of the bone. Hence, elastic modulus is an important aspect of a bone or implant when it is placed under load. Interestingly, the tensile strength of hard tissue bone does not match its compressive strength. Because compact and trabecular bones are different in structure, they have very different values for Young's Modulus of elasticity[50], as shown in Table 2. In a recent article, Reilly et. al also reported that the elastic moduli of human cortical bone in the longitudinal and transverse directions are typically in the range of 16–23 and 6–13 GPa, respectively[51]. Bone typically also exhibits R-curve behavior like other ceramic materials and experiences oblique, comminuted, spiral, compound, greenstick, transverse and simple types of fractures[52-54]. Hence, orthopedic application demands that the biocompatible prosthesis

material possess an excellent combination of elastic modulus, moderate fracture resistance, and compressive and tensile strength, with a reasonable growth factor. Therefore, synthetic biomaterials that are biocompatible, bioactive and capable of being tailored to mimic the mechanical properties of bone tissue may be advantageous for implant fixation, synthetic bone graft substitutes, tissue engineering scaffolds, and other orthopedic applications[55,56].

Section 3 demonstrates that the bone matrix is mainly composed of inorganic – organic constituents, which resembles the synthetic combination of HAp as an inorganic constituent and a biocompatible polymer with organic phase as an organic constituent. Among several candidate polymers, synthetic biocompatible polymers, including polyether ether ketone (PEEK) and high density polyethylene (HDPE), have been successfully reinforced with bioactive hydroxyapatite (HAp) for replacement or healing of bone. Similarly, the ultra-high molecular weight polyethylene (UHMWPE) is also employed in acetabular cups and several kinds of joints[57,58]. Hence, selection of polymer is mainly determined according to fulfillment of the physical properties of the composite or particular real life applications. A quick review of the characteristics of polymer and synthetic HAp can justify the material selection procedure and subsequent applications. For example, PEEK is a significantly low temperature synthetic polyaromatic semicrystalline thermoplastic polymer with a basic formula of $(–C_6H_4–O–C_6H_4–O–C_6H_4–CO–)_n$ having a melting temperature of 343^{o}C, a crystallization peak of 343^{o}C and a glass transition temperature of 143^{o}C. The high-temperature performance makes it a stable material in the human body[59]. In addition, its superior combination of strength, stiffness, toughness and elasto-plastic deformation, as well as outstanding chemical, hydrolysis and wear resistance, together with its extensive biocompatibility with collagen, have enabled it to be suitable for in-vitro load-bearing medical device applications. Moreover, PEEK is non-cytotoxic and can be repeatedly sterilized using conventional steam, gamma and ethylene oxide processes without evident degradation of its mechanical properties. Thus, it has become an option for long-term medical implants in orthopaedic, cardiovascular and dental markets[60,61]. Moreover, HDPE has a low degree of branching and, thus, stronger intermolecular forces and tensile strength. HDPE has a density of greater than or equal to 0.941g/cc with a melting temperature of 120-130^{o}C and an excellent chemical resistivity. Another high molecular weight polymer, UHMWPE, is less efficient in packing but possesses excellent toughness. On the other hand, synthetic nanocrystalline HAp is biocompatible with hard human tissues and possesses osteoconductive properties. The high-modulus HAp particle in biocomposites usually undergoes elastic deformation and seldom suffers crack failure during a load-bearing process[62]. However, the deformation behavior of the HAp reinforcement polymer biocomposite is able to satisfy the general Hooke's law [63].

The functions of composites are dependent on their chemical composition, processing conditions and microscale structure. Homogenization of insoluble ceramic-HAp phase within a polymer matrix is a challenging job. Except for filling the bone cavity, the shape and size of the bioimplant could be synchronized through several processes such as injection molding, compression molding and extrusion methods. Through injection molding (IM), up to 41vol% or 63wt% HAp phase can be homogenously dispersed within a PEEK matrix. Fortunately, this volume and percentage weight is well matched with the natural bone composition[6]. However, processing parameters such as melt temperature, residence time and cooling rate affect the crystallinity of the composites. Findings suggest that an increase in these parameters resulted in a decrease in crystallinity, which affects the composites' mechanical properties[64,65]. The processing details of the composite, which was prepared from spray-dried HAp powder with a density of 3.154gm/cc and a mean particle size of 19.94μm, are beyond the scope of this analysis and can be found in other studies[66]. Another group of researchers produced a 0-50vol% HAp dispersed PEEK composite through compression molding (CM), where the particle size of commercially available PEEK was 26μm[67]. More recently, a HAp whisker reinforced HDPE composite was produced through a conventional powder processing and compression molding technique, and exhibits acceptable mechanical properties when compared with bone[64]. Another interesting organic compound polyamide (PA) has a similar structure as bone collagen, while nanohydroxyapatite (n-HAp) has high surface activity and its size is similar to the mineral found in human hard tissues. In this context, Yubao et. al synthesized a novel composite HAp-PA/HDPE through a combined extrusion and injection molding method[68]. Table 3 shows a brief comparison of the mechanical properties of ceramic-polymer composites with those of natural human bone, where composites were prepared from different synthetic polymers by different processing techniques. The elastic modulus of HAP-PEEK composite exponentially increased with increasing HAp content when the specimen was prepared by the injection molding method. This is obvious since the moduli of HAp and PEEK are 85 and 3, respectively. Above 20% HAp content, the moduli exhibit a range of 4.3 to 11.4GPa, which falls within the low to middle range of the modulus of cortical bone. The modulus of HAp-PEEK could be altered with synchronization of the processing method and parameters. Roeder et. al illustrated that as-molded and annealed PEEK composites reinforced with 40vol% HAp whiskers exhibited elastic moduli in the order of 17GPa, which is a quite close to natural bone. They also pointed out how the anisotropy of mechnical properties of bone varied with the synthetic composites. Interestingly, 40vol% HAp reinforced HAp–PEEK composite exhibits a Vicker's microhardness of ~38VHN, which decreases up to ~12VHN with reduction of HAp (0 vol%) content. Similarly, the

compressive strength is also found to increase as the amount of HAp in the PEEK composite increases. In comparison to the compressive strength of cortical bone, which lies in the range of 106–215 MPa[67], PEEK polymer, by itself, has matching properties and can further be improved by progressive addition of HAp. For as-molded HAp-PEEK composite, there is a slight increase in tensile strength up to an additional 10vol% of HAp particles. Beyond this, however, tensile strength begins to decrease in almost a linear fashion[68]. The decrease is attributed to the weak adhesive interaction between the HA grain and the PEEK matrix. Additionally, to a lesser extent, cohesive failure could also be noticed through fracture of the HAp grain. The tensile strength of the HAp-PEEK composite ranged from 49.0 to 83.3MPa; indicates the lower limits of tensile strength of cortical bone[69]. A similar trend could be observed for the compression molded specimens. However, the tensile strength of the compression molded specimens was higher than that of the injection molding specimens. PEEK reinforced with 30–50 vol% HA whiskers exhibits virtually no plastic deformation. PEEK matrix phase dramatically increases elastic modulus and ultimate tensile strength, but reduces work-to-failure compared to HAp whisker-reinforced HDPE. HAp-whisker-reinforced HDPE achieved an elastic modulus similar to the transverse direction of human cortical bone, in the range of 9 – 11GPa, while HAp-whisker-reinforced PEEK exhibited an elastic modulus similar to that of human cortical bone in the longitudinal direction, within the range of 17 – 23GPa at similar reinforcement levels[64]. Similarly, the ultimate tensile strength has been dramatically improved, up to three-fold, using PEEK, compared to HDPE, at similar reinforcement levels. The inferior mechanical properties of the HDPE matrix limited the application of these composites to non-load-bearing devices[70]. The adhesive force within reinforced particulate and organic material is noticeably improved when nano-HAp particles act with the polar group of PA polymer. Such adhesion could undergo large local deformation, resulting in the high mechanical strength of the composite. As a result, most of the mechanical properties improved in the presence of nano-HAp phase. However, a higher content of HAp (50% weight fraction) enhances the agglomeration and decreases the mechanical strength[64]. A similar trend could also be observed for other ceramic phases[71]. A recently investigated HA-UHMWPE nanocomposite exhibits a modulus value two orders higher in the range of 4GPa as compared to UHMWPE[57]. The bending strength (25-66 MPa) and fracture toughness of a MWCNTs/HAp composite sintered in a vacuum or in Ar together with heat treatment are also higher than those of pure hydroxyapatite. The increment of the fracture toughness is most obvious and its maximum value reaches up to 2.4 $MPam^{1/2}$, which is about eight times higher than that of pure HAp, but only about half that of human bone[72].

To justify the mechano-transduction effect of bone, Jianqing et. al developed a novel biocompatible Hydroxyapatite – Barium Titanate (HABT) composite, which exhibits significant

osteogenesis in comparison to HAp phase alone[73]. This can presumably be attributed to the piezoelectric properties of biocompatible nano-$BaTiO_3$ phase. They also demonstrated that the tissue growth on the surface vertical to the polarized direction is faster than that on the surface parallel to the polarized direction. However, detailed study on piezoelectric effects is required to understand the bone growth mechanism. The composite exhibits mechanical properties of a lower order of magnitude than those of the human femur. This shortcoming may be overcome through proper combination with a polymer matrix.

This brief analysis illustrates that an appropriate ceramic-polymer composite could be an acceptable alternative material for use as prosthetic bone in terms of accommodating growth and maintaining the necessary physical properties. Moreover, selection of material and synchronization of properties are clearly key elements for the further development of bone implants or bone repair materials.

8. Concluding Remarks

The similarities between the elastic modulus, compressive strength and tensile strength of human cortical bone and HAp-whisker-reinforced polymer composite suggests the latter as a probable candidate for orthopedic implants which may bear physiological levels of load. Osteogenesis under mechanical loading and osteoconductivity could be controlled through the addition of nano-HAp phase. Hence, a good understanding of relevant material selection can inform the search for new strategies in bone tissue engineering and the transplantation of next-generation biomaterials.

References

1. S.L. Rothman, W. Glenn, M. Rhodes, R. Brucc, C. Pratt, “Individualized prosthesis production from routine CT data,” *Radiology* **157** 177 (1985).
2. F. Minutoli, M. Gaeta, A. Bottari and A. Blandino, “MRI findings in regional migratory osteoporosis of the knee migrating from the femur to the tibia,” *Clinical Imaging* **30** 428-430 (2006).
3. S.C. Cowin, W.C. Van Buskirk, R.B. Ashman, “Properties of bone. In: Skalak R, Chien S, editors. Handbook of Bioengineering”; pp. 26-30, *New York: McGraw-Hill*, 1987.
4. L. Mosekilde, “Vertebral structure and strength in vivo and in vitro,” *Calcif Tissue Int*, **53** S121–6 (1993).
5. M.C. Van der Meulen, K.J. Jepsen, B. Mikic, “Understanding bone strength: size isn't everything,” *Bone* **29** 101–4 (2001).
6. L. Hench, “Bioceramics: From Concept to Clinic”, *J. Am. Ceram. Soc*, **74** 1487-510 (1991).
7. W. Bonefield, “Hydroxyapatite Reinforced Polyethylene as an Analogous Material for Bone Replacement,” Am. Acad. Sci., **523** 173 (1988).
8. W. Bonefield, “Composites for Bone Replacement,” *J. Biomed. Eng.*, **10** 522 (1998).
9. F.G. Evans, R.L. Herbert, “Tensile and Compressive Strength of Human Parietal Bone,” *J Appl Physiol* **104** 93-497 (1957).
10. J.D. Currey, “The relationship between the stiffness and the mineral content of bone,” *J. Biomech* **2** 477-80 (1969).
11. J.D. Currey, “Physical characteristics affecting the tensile failure properties of compact bone,” *J Biomech*, **23** 837–844 (1990).
12. B.G. Stuart, Ting M, Richard C, Ravi R, Smith RL. “Effects of orthopaedic wear particles on osteoprogenitor cells,” *Biomaterials*, **27** 6096–6101 (2006).
13. D.P. Pioletti, A. Kottelat, “The influence of wear particles in the expression of osteoclastogenesis factors by osteoblasts,” *Biomaterials*, **25** 5803–5808 (2004).
14. E. Fukada, “Piezoelectricity of bone and osteogenesis by piezoelectric films. In: Becker RO, editor. Mechanisms of Growth Control”, *Springfield: Thomas*, 192-210 (1981).
15. A.A. Marino, J. Rosson, E. Gonzalez, L. Jones, S. Rogers, E. Fukada, “Quasi-static charge interactions in bone,” *J. Electrostat* **21** 347-360 (1988).
16. M. Otter, J. Shoenung, W.S. Williams, “Evidence for different sources of stress-generated potentials in wet and dry bone,” *J. Orthop. Res* **3** 321-324 (1985).

17. H. Macdonald, S. Kontulainen, M. Petit, P. Janssen, H. McKay, “Bone strength and its determinants in pre- and early pubertal boys and girls,” *Bone* **39** 598-608 (2006).
18. L.Y. Griffin, “Noncontact ACL Injuries: risk factors and prevention strategies,” *J. Am. Acad. of Orth. Surg*, **8** 141-150 (2000).
19. H. Gray, “Anatomy of the human body”. pp 95-96, In: Warren HL, editor. Philadelphia: Lea & Febriger, 1918.
20. S. Mohsin, F.J. O'Brien, T.C. Lee, “Osteonal crack barriers in ovine compact bone,” *J. Anatomy* **208** 81–89 (2006).
21. S. Weiner, W. Traub, “Bone structure: from angstroms to microns,” *The FASEB,* **6** 879-885 (1992).
22. S.Lees, “A model for the distribution of HAP crystallites in bone - a hypothesis,” *Calcif. Tiss. Int.*, **27** 53-56 (1976).
23. L. Cristofolini, M. Viceconti, A. Cappello, A. Toni, “Mechanical validation of whole bone composite femur models,” *J. Biomech*, **29** 525-535 (1996).
24. W.S.S. Jee, “The skeletal tissues” pp 206-254, In: Weiss L. editor. Histology: cell and tissue biology. 5th edition 1983.
25. J. Wolff, “The law of bone remodeling”; Berlin: Springer Verlag. 1986.
26. K.D. Rogers, P. Zioupos, “The bone tissue of the rostrum of a Mesoplodon Densirostris whale: a mammalian biomineral demonstrating extreme texture,” *J Mater Sci Lett,* **18** 651-654 (1999).
27. G. Marotti, M.A. Muglia, “A scanning electron microscope study of human bony lamellae. Proposal for a new model of collagen lamellar organization,” *Arch. Ital. Anat. Embriol,* **93** 163-175 (1988).
28. L.L. Hench, E.C. Ethridge, “An Interfacial Approach, Biomaterials,” pp 345-346, New York: Academic Press 1982.
29. H.C.W. Skinner, Mineral and human health. *In* Environmental Mineralogy. pp 383–412, EMU Notes in Mineralogy 2. D. J. Vaughan and R. A. Wogelius, editors. Eötvös University Press, Budapest, 2000.
30. F.C.M. Driessens, R.M.H. Verbeeck, Biominerals, pp 179-209, FL: CRC Press, Boca Raton, 1990.
31. M.C. Dalconi, C. Meneghini, S. Nuzzo, R. Wenk, S. Mobilio, “Structure of bioapatite in human foetal bones: An X-ray diffraction study,” Nuclear Instruments and Methods in Physics Research B **200** 406–410 (2003).
32. http://www.pentax.jp/english/lifecare/newceramics/apaceram/index.html

33. H. Stöss, P. Freisinger, "Collagen fibrils of osteoid in osteogenesis imperfecta: morphometrical analysis of the fibril diameter," *Am. J. Med.Gen*., **45** 257 (1993).
34. T. Miyata, T. Taira, Y. Noishiki, "Collagen Engineering for Biomaterial Use," *Clinical Mater,* **9** 139-148 (1992).
35. J. Jonas, J. Burns, E.W. Abel, M.J. Cresswell, J.J. Strain, C.R. Paterson, "Impaired mechanical strength of bone in experimental copper deficiency," *Ann Nutr Metab,* **37** 245–52 (1993).
36. E. Fukada, I. Yasuda, "On the piezoelectric effect of bone," *J. Phys. Soc. Japan,* **12** 1158-1162 (1957).
37. A.J. Grodzinsky, H. Lipshitz, M.J. Glimcher, "Electromechanical properties of articular cartilage during compression and stress relaxation," Nature, **275** 448-450 (1978).
38. G.B. Reinish, A.S. Nowick, "Piezoelectric Properties of Bone as Functions of moisture content," *Nature,* **253** 626 -627 (1975).
39. D. Hilmi, G. Nejat, "A mixture model for wet bones—I theory," *Inter J Eng Sci,* **15** 707-718 (1977).
40. A. Wang, V.K. Poineni, A. Essner, M. Sokol, D.C. Sun, C. Stark, J.H. Dumbleton, "The significance of nonliniear motion in the wear screening of orthopaedic implant materials," *J Testing Eval,* **25** 239-245 (1997).
41. D. Sarkar, S.J. Cho, M.C. Chu, S.S. Hwang, S.W. Park, B. Basu, "Tribological properties of Ti_3SiC_2," ***J*** *Am Ceram Soc*, **88** 3245–3248 (2005).
42. D. Sarkar, B. Basu, M.C. Chu, S.J. Cho, "Is glass infiltration beneficial to improve Fretting wear Properties for Alumina?" *J. Am. Ceram. Soc.,* **90** 523–532 (2007).
43. K.E. Healy, P. Ducheyne, "Passive Dissolution of Titanium in Biological Environments (Review)," In: Brown, SA Lemons JE, editors. Medical Applications of Titanium and its Alloys: the Material and Biological Issues. Philadelphia: ASTM STP, 1996.
44. R.V. Noort, "Review Titanium: the Implant Material of Today," *J. Mater. Sci*., **22** 3801-81 (1987).
45. L.Z. Zhuang, E.W. Langer, "Determination of cyclic strain-hardening behaviour produced during fatigue crack growth in cast Co-Cr-Mo alloy used for surgical implants," *Mater. Sci. Eng. A*, **108** 247-252 (1989).
46. X. Wang, Y.Li, J. Wei and k. Groot, "Development of Biomimetic Nano-hydroxyapatite/poly (Hexamethylene Adipamide) Composites," *Biomaterials*, **23** [9] 4787 (2002).

47. S. Hasegawaa, S. Ishii, J. Tamura, T. Furukawa, M. Neo, Y. Matsusueb, Y. Shinkinami, M. Okuno and T. Nakamura, " A 5-7 year in vivo Study of High-strength Hydroxyapatite/poly(L-lactide) Composite Rods for the Internal Fixation of Bone fractures," *Biomaterials*, **27** 1327-32 (2006).
48. H. Itokawa, T. Hiraide, M. Moriya, M. Fujimoto, G. Nagashima, R. Suzuki and T. Fujimoto, "A 12 Month in vivo study of the response of Bone to a Hydroxyapatite-Polymethylmethacrylate Cranioplasty Composite," Biomaterials, **28** 4922-27 (2007).
49. F.R.A.J. Rose, R.O.C. Oreffo, "Bone tissue engineering: hope vs. hype," *Biochem Biophys Res Commun*, **292** 1–7 (2002).
50. D.T. Reilly, A.H. Burstein, V.H. Frankel,"The elastic modulus of bone," *J. Biomechanics*, **7** 271-275 (1974).
51. D.T. Reilly, A.H. Burstein, "The elastic and ultimate properties of compact bone tissue," *J Biomech*, **8** 305–93 (1975).
52. D. Sarkar, B. Basu, M.C. Chu, S.J. Cho, "R-Curve Behavior of Ti_3SiC_2," *Ceram Inter*, **33** 789 -793 (2007).
53. R.K. Nalla, J.J. Kruzic, J.H. Kinney, R.O. Ritchie, "Mechanistic aspects of fracture and R-curve behavior in human cortical bone," *Biomaterials*, **26** 217-231 (2005).
54. A. Kolleck, G.A. Schneider, F.A. Meschke, "R-curve behavior of $BaTiO_3$- and PZT ceramics under the influence of an electric field applied parallel to the crack front," *Acta Mater*, **48** 4099-4113 (2000).
55. K.E. Tanner, R.N. Downes, W. Bonfield, "Clinical applications of hydroxyapatite reinforced materials," *Br Ceram Trans*, **93** 104–107 (1994).
56. M. Wang, R. Joseph, W. Bonfield, "Hydroxyapatite–polyethylene composites for bone substitution: effects of ceramic particle size and morphology," *Biomaterials*, **19** 2357–2366 (1998).
57. L. Fang, Y. Leng, P. Gao, "Processing and mechanical properties of HA/UHMWPE nanocomposites," *Biomaterials*, **27** 3701–7 (2006).
58. W. Pompe, H. Worch, M. Epple, W. Friess, M. Gelinsky, P. Greil, U. Hempel, D. Scharnweber, K. Schulte, "Functionally graded materials for biomedical applications," *Mater Sci Eng A*, **362** 40–60 (2003).
59. M.S.A. Bakar, K. Cheang, A. Khor, "Thermal processing of hydroxyapatite reinforced polyetheretherketone composites," *J Mater Proc Tech*, **89-90** 462-466 (1999).

60. F.N. Cogswell, D.C. Leach, “Thermoplastic structural composites in service,” Plastics, Rubber and Composites Processing and Applications, **18** 249 (1992).
61. K. Fujihara, K. Teo, R. Gopal, P.L. Loh, V.K. Ganesh, S. Ramakrishna, K.W.C. Foong, C.L. Chew, “Fibrous composite materials in dentistry and orthopaedics: review and applications,” *Comp Sci Tech,* **64** 775–788 (2004).
62. A.A. Corvelli, P.J. Biermann, J.C. Roberts, “Design, analysis and fabrication of a composite segmental bone replacement implant,” *J Adv Mater*, **2** 2–8 (1997).
63. D.J. Kelsey, G.S. Springer, “Composite implant for bone replacement,” *J Compos Mater,* **31** 1593–631 (1997).
64. R.K. Roeder, M.M. Sproul, C.H. Turner, “Hydroxyapatite whiskers provide improved mechanical properties in reinforced polymer composites,” *J Biomed Mater Res,* **67A** 801–812 (2003).
65. M. Akay, N. Aslan, “Polymeric composite hip-joint prosthesis,” *Adv Compos Lett*, **1** 74–6 (1992).
66. M. S.A. Bakar, P. Cheang, K.A. Khor, “Mechanical properties of injection molded hydroxyapatite polyetheretherketone Biocomposites,” Comp Sci Tech, **63** 421–425 (2003)
67. G.L. Converse, W. Yue, R.K. Roeder, “Processing and tensile properties of hydroxyapatite-whisker-reinforced polyetheretherketone,” *Biomaterials,* **28** 927–935 (2007).
68. Y. Zuo, Y. Li, J. Li, X. Zhang, H. Liao, Y. Wang, W. Yang, “Novel bio-composite of hydroxyapatite reinforced polyamide and polyethylene: Composition and properties,” *Mater Sci Eng A,* **452-453** 512-517 (2006)..
69. X.E. Guo, “Mechanical properties of cortical and cancellous bone tissue,” pp 10.5–10.14, In: Cowin SC, editor. Bone mechanics handbook. 2nd ed. Boca Raton, FL: CRC Press LLC; 2001.
70. M. Wang, N.H. Ladizesky, K.E. Tanner, I.M. Ward, W. Bonfield, “Hydrostatically extruded HAPEXTM,” *J Mater Sci,* **5** 1023–1030 (2000).
71. D. Mohapatra, D. Sarkar, “Preparation of MgO-$MgAl_2O_4$ Composite for Refractory Application,” *J Mater Proc Tech,* **189** 279-283 (2007).
72. L. Aimin, S. Kangning, D. Weifang, Z. Dongmei, “Mechanical properties, microstructure and histocompatibility of MWCNTs/HAp biocomposites,” Mater Lett, **61** 1839-1844 (2006).
73. F. Jianqing, Y. Huipin, Z. Xingdong, “Promotion of osteogenesis by a piezoelectric biological ceramic,” Biomaterials, **18** 1531-1534 (1997).

List of Tables

Table 1. Comparison of the structural features of cortical and trabecular bone[24]

Structural Feature	Cortical Bone	Trabecular Bone
Volume Fraction (mm^3/mm^3)	0.80 (0.85 – 0.95)	0.20 (0.05 – 0.60)
Surface/Bone Volume (mm^2/mm^3)	2.5	20
Total Bone Volume (mm^3)	1.4×10^6	0.35×10^6
Total Internal Surface (mm^2)	3.5×10^6	7.0×10^6

Table 2: Tensile, Compressive Strength and Young's Modulus for Compact and Trabecular Bone[50]

Type of Bone	Compressive Breaking Stress (N/mm^2)	Tensile Breaking Stress (N/mm^2)	Young's Modulus ($10^2 N/mm^2$)
Compact	170	120	179
Trabecular	2.2	-	0.76

Table 3: Comparative mechanical properties of ceramic-polymer composite for bone scaffold

Material	Elastic Modulus (GPa)	Compressive Strength (MPa)	Tensile Strength (MPa)	Ref
HAp-PEEK [Polyetheretherketone, $(–C_6H_4–O– C_6H_4–O–C_6H_4–CO–)_n$]				IM[66],
HAp (0 Vol%)	3.0 (IM), 4.7	113 (IM)	79.6 (IM), 100.0(CM)	CM[64]
(10 Vol%)	3.3 (IM), 7.3 4.3 (IM), 9.5 8.5 (IM), 13.0 11.4 (IM), 17.0	125 (IM) 139 (IM) - -	83.3 (IM), 62.8 (IM), 60.2 (IM), 49.0 (IM),	
(20 Vol%)	23.0 (CM)	-	44.5(CM)	
HAp-HDPE (High Density Polyethylene)				CM[64]
HAp (10 Vol%)	2.2 (CM)	-	27.0 (CM)	
	4.8 (CM)	-	29.0 (CM)	
(20 Vol%)	8.9 (CM)	-	22.5 (CM)	
	11.3 (CM)	-	20.4 (CM)	
HAp-PA (Polyamide) /HDPE				EM+IM[68]
HAp (0 Wt%)	5.0 (EM+IM)	45 (EM+IM)	25.0 (EM+IM)	
(20 Wt%)	4.5 (EM+IM)	55 (EM+IM)	35.2 (EM+IM)	
	5.0 (EM+IM)	62 (EM+IM)	30.5 (EM+IM)	
(40	6.0 (EM+IM)	58 (EM+IM)	22.8 (EM+IM)	
Compact Bone (Human)	16-30 (longitudinal) 6-13 (transverse)	106 – 215	50 – 150	[51]

IM = Injection Molding, CM = Compression Molding, EM = Extrusion Mechanics

List of Figures:

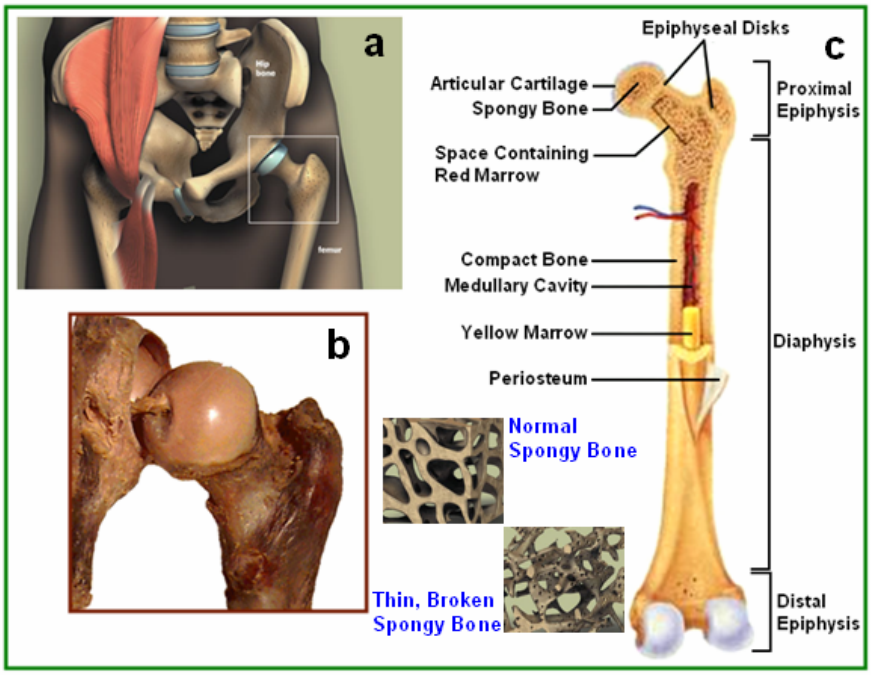

Fig 1: Anatomy of femur: a) a schematic representation of the hip bone, b) the ball-and-socket joint of a femur attached through a ligament and c) a detail histology of the femur where the spongy bone exhibits a large range of porosity[19].

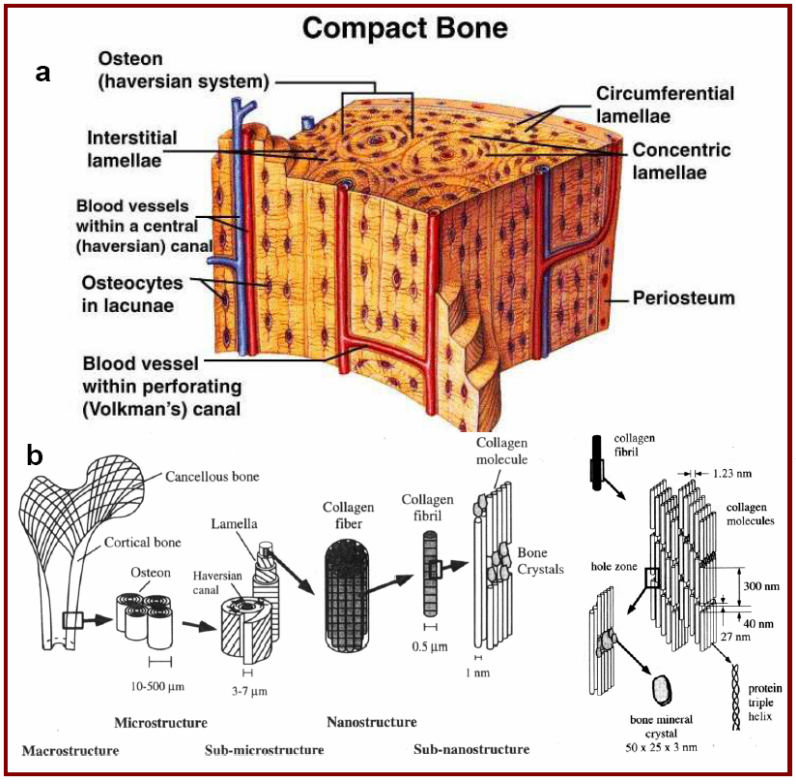

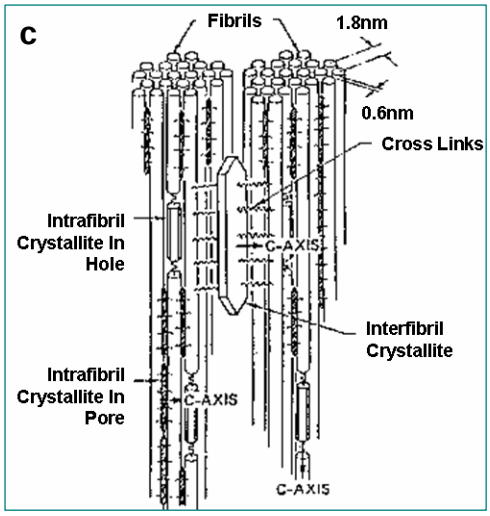

Fig 2: Typical compact bone with Haversian system (a), schematic view of the orientation of collagen and HAp crystal within bone matrix (b) and preferred mode of orientation along the longitudinal direction[19,22]

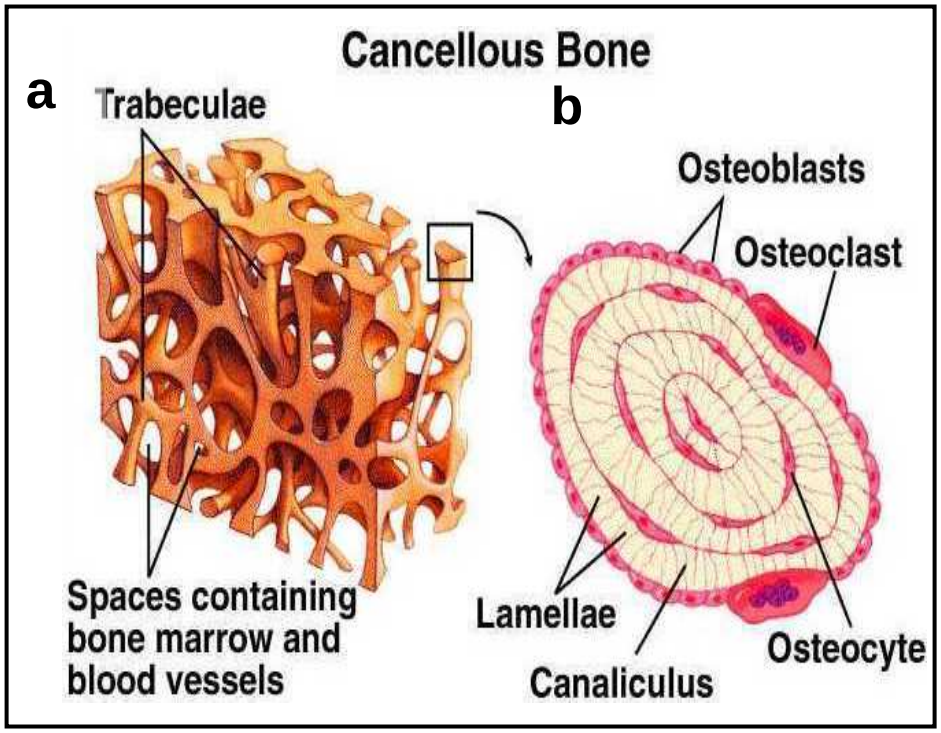

Fig 3: Porous trabeculae bone (a) with osteon bone (b) [19,23].

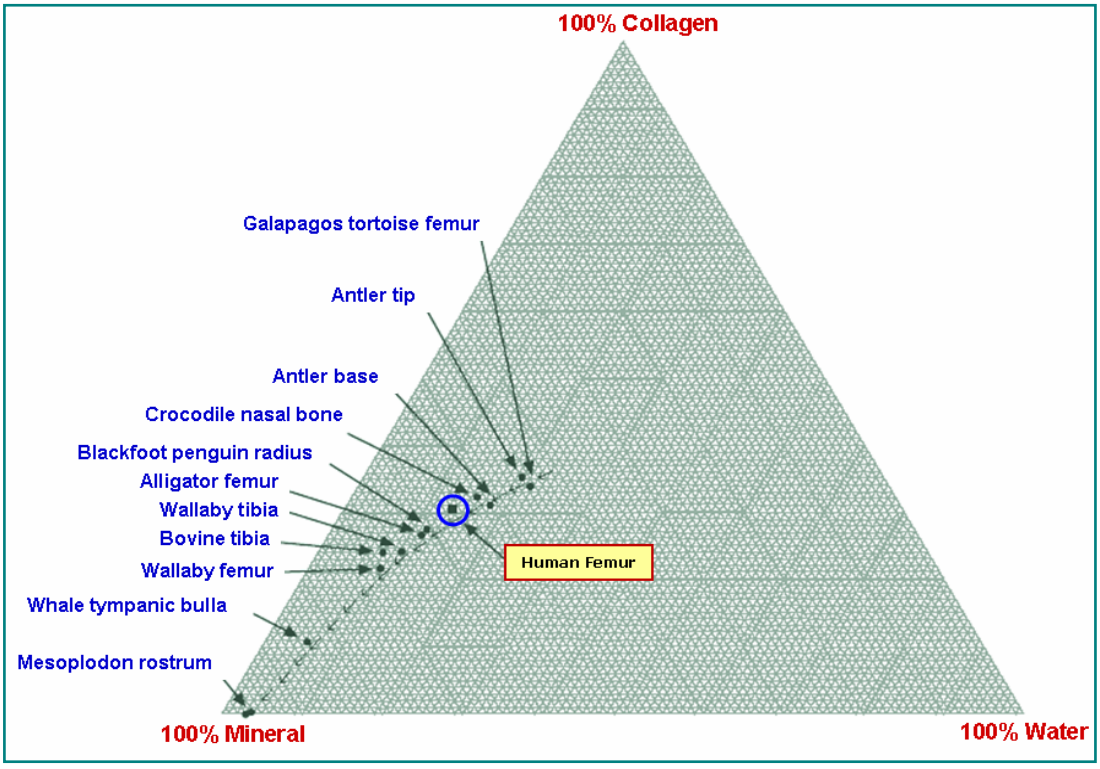

Fig 4: Ternary diagram showing the mineral, collagen and water fractions of different bone tissues[26]

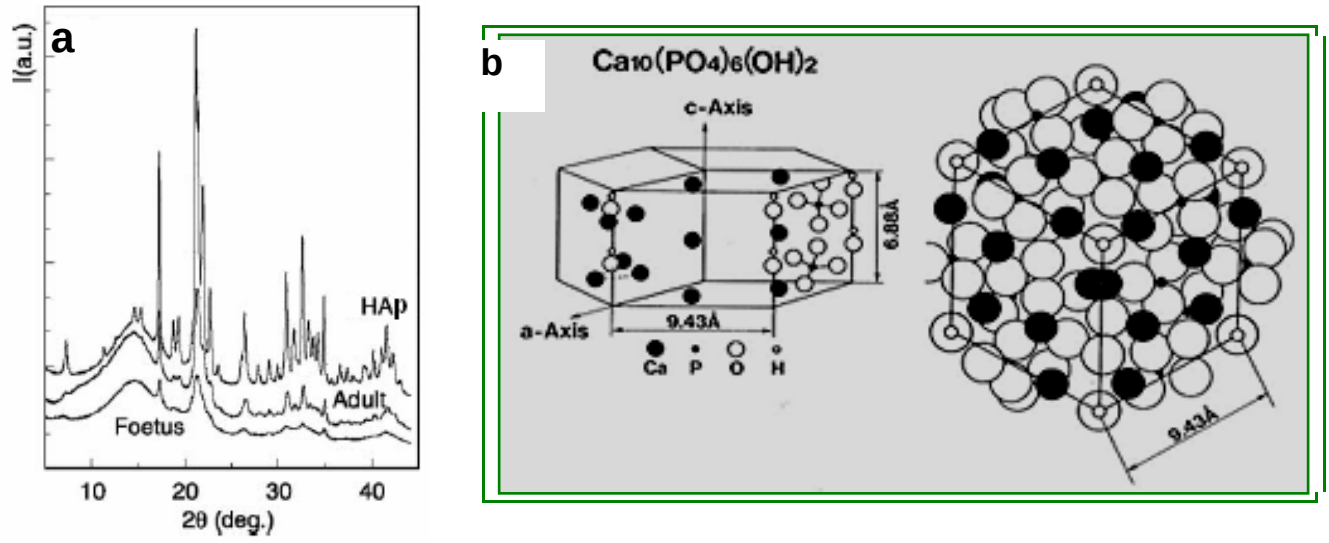

Fig 5: (a) Comparative XRD patterns of foetal bone, adult bone and synthetic HAp (b) typical Crystal structure of HAp[31,32].

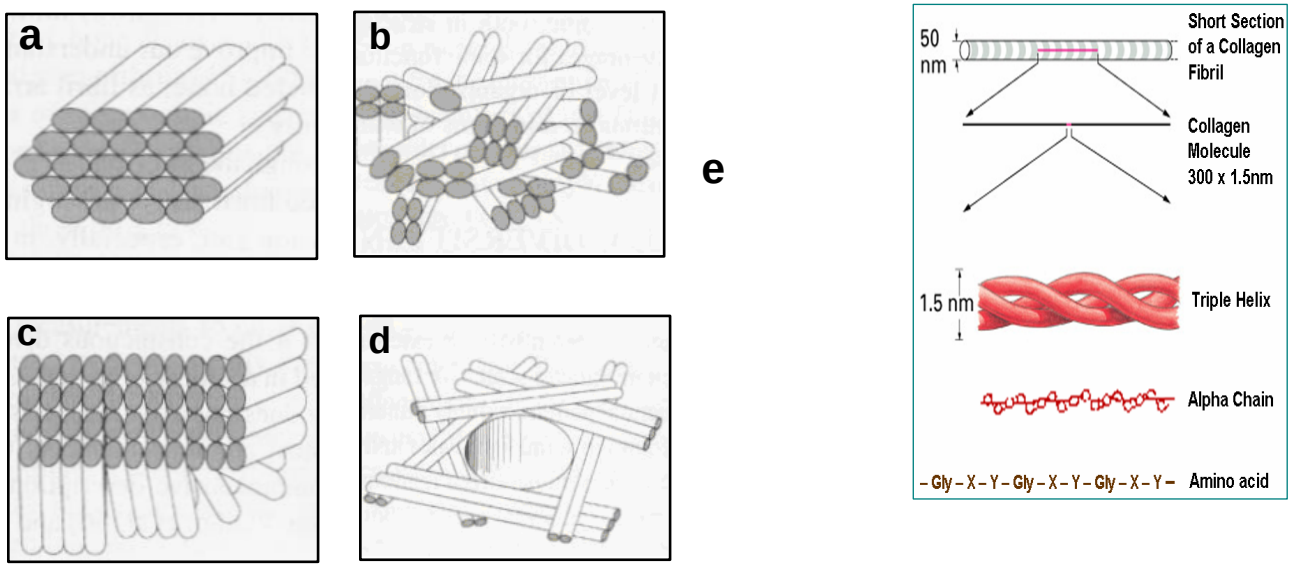

Fig 6: Schematic of fibril array pattern: (a) parallel fibrils, (b) woven fiber structure, (c) plywood-like structure, (d) radial fibril arrays and (e) the structure and orientation of collagen[33,34].